Research Square

Preprints are preliminary reports that have not undergone peer review.
They should not be considered conclusive, used to inform clinical practice,
or referenced by the media as validated information.

# Osimertinib-induced cardiopulmonary toxicity: a network toxicology, molecular docking, and molecular dynamics simulation study

**Huihui Yang**
Wenling Hospital of Traditional Chinese Medicine
**Jiajia Shao**
Wenling Maternal and Child Health Care Hospital
**Jiawei Han**
Wenling Maternal and Child Health Care Hospital
**Enfu Tao**
wenling Maternal and Child Health Care Hospital
**Jiayi Zhong**
abc1481376220163.com

Wenling Maternal and Child Health Care Hospital

**Article**

**Keywords:** Osimertinib, Cardiotoxicity, Pulmotoxicity, Network toxicology, Molecular docking, Molecular dynamics simulations

**Posted Date:** November 13th, 2026

**DOI:** https://doi.org/10.21203/rs.3.rs-11304777/v1

**License:** This work is licensed under a Creative Commons Attribution 4.0 International License.
Read Full License

**Additional Declarations:** No competing interests reported.

# Osimertinib-induced cardiopulmonary toxicity: a network toxicology, molecular docking, and molecular dynamics simulation study

Huihui Yang[1], Jiajia Shao[2], Jiawei Han[2], Enfu Tao[3,4], *Jiayi Zhong[2, *]

1 Department of Pharmacy, Wenling Hospital of Traditional Chinese Medicine, Wenling, Zhejiang Province, China.

2 Department of Pharmacy, Wenling Maternal and Child Health Care Hospital, Wenling, Zhejiang Province, China.

3 Department of Neonatology and NICU, Wenling Maternal and Child Health Care Hospital, Wenling, Zhejiang Province, China.

4 Department of Science and Education, Wenling Maternal and Child Health Care Hospital. Wenling, Zhejiang Province, China.

*Correspondence:Jiayi Zhong.

Department of Pharmacy, Wenling Maternal and Child Health Care Hospital, 102 Xiabao Road, Chengdong Street, Wenling, Zhejiang Province, China, 317500. Tel: +86-0576-86168367; Fax: +86-0576-86168022; E-mail: abc148137622@163.com

## Abstract

**Context:** Osimertinib, a third-generation epidermal growth factor receptor (EGFR) tyrosine kinase inhibitor, is first-line therapy for EGFR T790M mutation-positive non-small cell lung cancer (NSCLC). However, its clinical utility is severely limited by significant cardiotoxicity and pulmotoxicity, which compromise treatment adherence and patient survival. The shared molecular pathogenesis underlying these concurrent adverse effects remains unclear and warrants systematic investigation.

**Methods:** We employed an integrated computational framework combining network toxicology, molecular docking, and molecular dynamics (MD) simulations. Multi-database screening identified 119 shared targets between osimertinib and cardiopulmonary toxicity, from which seven hub targets—TP53, ESR1, HDAC1, CREBBP, EP300, HDAC2, and SMARCA4—were prioritized. Enrichment analysis implicated these targets in epigenetic regulation and cancer-related pathways such as microRNAs in cancer. Molecular docking confirmed high-affinity binding of osimertinib to all hub targets (binding free energies -6.4 to -7.2 kcal/mol). MD simulations demonstrated stable binding with HDAC1 and

CREBBP (-20.85 and -22.92 kcal/mol, respectively) and identified key interacting residues. This work outlines a multi-target, multi-pathway regulatory network and proposes an epigenetics-centered hypothesis: osimertinib-induced cardiopulmonary toxicity may arise from disruption of the CREBBP/EP300-HDAC1/HDAC2 epigenetic balance together with TP53-, ESR1-, and SMARCA4-mediated interactions, providing a theoretical basis for future experimental validation and therapeutic modulation.

**Keywords** Osimertinib·Cardiotoxicity·Pulmotoxicity·Network toxicology·Molecular docking·Molecular dynamics simulations

**Abbreviations**

NSCLC = Non-small cell lung cancer, EGFR = epidermal growth factor receptor, TKIs = tyrosine kinase inhibitors, ILD = drug-related interstitial lung disease, MDS = molecular dynamics simulations, OMIM = Online Mendelian Inheritance in Man, TTD = Therapeutic Target Database, GO = Gene Ontology, KEGG = Kyoto Encyclopedia of Genes and Genomes, BP = biological process, MF = molecular function, CC = cellular component, PDB = Protein Data Bank, BE = binding energy, RMSD = Root mean square deviation, Rg = radius of gyration, RMSF = root mean square fluctuation, HB = hydrogen bond, SASA = solvent accessible surface area, FEL = free energy landscape, PCA = principal component analysis, MMPBSA = Molecular Mechanics Poisson-Boltzmann Surface Area

## Introduction

Non-small cell lung cancer (NSCLC) represents a leading cause of cancer-related mortality worldwide, accounting for approximately 85% of all lung cancer cases[1]. Presently, various therapeutic approaches are employed in the management of NSCLC, including surgical intervention, radiotherapy, chemotherapy, immunotherapy, and targeted therapy, among others[2]. Despite surgical treatment, a significant proportion of patients remain at risk for distant metastasis or local recurrence[3]. With ongoing, in-depth research into the molecular mechanisms underlying lung cancer, targeted therapy has emerged as a central treatment strategy for NSCLC. The epidermal growth factor receptor (EGFR) plays a pivotal role in the pathogenesis of NSCLC[4]. Based on the research of EGFR, multiple generations of EGFR tyrosine kinase inhibitors (TKIs) have been developed and are currently used in clinical practice[5]. The first and second generations of EGFR inhibitors are extensively applied as

first-line treatments for advanced NSCLC characterized by EGFR-sensitive mutations[6]. Nevertheless, clinical practice shows that a subset of patients who have received first-line treatment with first or second-generation EGFR-TKIs will inevitably develop drug resistance[5], posing significant challenges for subsequent therapeutic interventions. Osimertinib, a third-generation EGFR-TKI, is specifically designed to target the T790M mutation and exhibits high selectivity in its action[7, 8]. This agent has demonstrated efficacy in overcoming the drug resistance associated with first and second-generation TKIs[9, 10]. Currently, osimertinib has received approval for the treatment of adult patients with locally advanced or metastatic NSCLC who are positive for the EGFR T790M mutation and have experienced disease progression during or following EGFR-TKI therapy[11].

With the increasing clinical application of osimertinib, concerns regarding its potential toxicity have become more prominent. An investigation utilizing data from the Italian pharmacovigilance database assessed the safety profile of TKIs from 2006 to 2021[12]. The results indicate that common adverse reactions associated with TKIs predominantly include dermatological issues, gastrointestinal discomfort, hepatic dysfunction, respiratory disorders, and infections. Nonetheless, more severe and potentially life-threateningadverse drug reactions, such as respiratory failure, interstitial lung disease, and cardiogenic shock, necessitate vigilant monitoring, particularly in younger patients. Compared to other TKIs, osimertinib exhibits a heightened propensity for inducing cardiac-related adverse events, including QT interval prolongation, atrial fibrillation, reduced left ventricular ejection fraction, and heart failure[13]. Cardiotoxicity has been recognized as a relatively common adverse effect of osimertinib in both phase III clinical trials[14] and real-world studies[15]. Severe cases (grade≥3) are not infrequent and, in certain instances, may lead to patient mortality.

In addition to cardiac toxicity, the pulmonary toxicity associated with osimertinib, particularly drug-related interstitial lung disease (ILD), has garnered significant attention. ILD serves as an umbrella term encompassing a diverse array of heterogeneous conditions primarily characterized by lesions within the pulmonary interstitium[16]. These conditions are marked by non-infectious inflammatory alterations in either focal or diffuse patterns within the pulmonary interstitium, leading to pathological changes that may ultimately result in respiratory failure and cardiac insufficiency[8]. Although ILD is considered a rare and potentially fatal adverse event linked to osimertinib, real-world data indicate a higher incidence than previously anticipated. In a cohort of 583 patients undergoing first-line osimertinib therapy, 75 patients (12.8%) developed ILD, with 18 patients (3.0%) experiencing

at least grade 3 ILD[17]. Furthermore, a multicenter study involving 452 patients reported an incidence of drug-related pneumonitis at 18%, with 4.6% classified as grade≥3. Among these patients, some exhibited transient asymptomatic pulmonary opacities, while others manifested more severe inflammatory responses, including organizing pneumonia, eosinophilic pneumonia, allergic pneumonitis, and diffuse alveolar damage[18].

In clinical practice, we encountered a case in which osimertinib induced simultaneous cardiopulmonary toxicity, and such an adverse reaction has endangered the health of the patient. Nonetheless, the molecular mechanisms underlying the simultaneous occurrence of cardiopulmonary toxicity remain inadequately understood, which impedes early identification and targeted prevention strategies in at-risk populations. Although instances of osimertinib-induced cardio-pulmotoxicity have been documented independently, the exploration of their common molecular triggers has not been undertaken in the existing literature. Network toxicology, an emerging interdisciplinary framework that integrates systems biology, toxicogenomics, and computational pharmacology, offers substantial advantages for the investigation of complex drug-induced toxicities[19]. By constructing comprehensive “drug-target-toxicity” interaction networks, network toxicology facilitates the identification of shared molecular targets and signaling pathways[20]. Despite its established efficacy in toxicity prediction, no studies to date have employed network toxicology to investigate the dual mechanisms of osimertinib-induced cardio-pulmotoxicity, thereby highlighting a critical gap in the current body of knowledge.

In the present study, our primary objective was to elucidate the underlying mechanisms by which osimertinib induces cardiopulmonary toxicity. To achieve this goal, we employed a multidisciplinary approach that integrated network pharmacology, bioinformatics, and molecular dynamics simulations (MDS) to systematically identify and characterize key therapeutic targets and biological pathways. To the best of our knowledge, this investigation represents the first application of network pharmacology and MDS to explore molecular mechanisms of osimertinib's cardiopulmonary adverse effects. Our current study has not only explained the theoretical basis of cardiopulmonary toxicity induced by osimertinib but has also provided insights into mechanism-oriented targeted intervention strategies that could effectively reduce the harm from adverse reactions.

**Materials and methods**

**Disease-related targets for cardiotoxicity and pulmotoxicity**

Potential targets associated with cardiotoxicity and pulmotoxicity were retrieved from three publicly available databases, including the GeneCards database (http://www.genecards.org/, accessed on June 15, 2025) (Relevance score probability ≥ 10[21], the Online Mendelian Inheritance in Man database[22] (OMIM, http://www.omim.org/, accessed on June 15, 2025), and the Therapeutic Target Database[23] (TTD, http://db.idrblab.net/ttd/, accessed on June 15, 2025). All searches were performed with the keywords "cardiotoxicity OR heart failure OR QT prolongation OR cardiac arrhythmia OR atrial fibrillation OR cardiomyopathy OR pericardial effusion OR left ventricular dysfunction OR myocarditis" and "interstitial pneumonia OR interstitial lung disease OR pneumonitis OR pneumonia OR pneumothorax". After merging and removing duplicate targets, disease-related targets for cardiotoxicity and pulmotoxicity were finally determined.

**Drug targets for osimertinib**

The standard structure and SMILE notation of osimertinib were retrieved from the PubChem database (https://pubchem.ncbi.nlm.nih.gov, accessed on June 17, 2025). Potential protein targets of osimertinib were predicted using three platforms: ChEMBL[24] (https://www.ebi.ac.uk/chembl, accessed on June 17, 2025), STITCH (http://stitch.embl.de/, accessed on June 17, 2025), and Swiss Target Prediction (https://www.swisstargetprediction.ch/, accessed on June 17, 2025)[25]. All searches were restricted to *Homo sapiens*. For SwissTargetPrediction, a probability threshold of >0.1 was applied to enhance prediction reliability[26]. After integrating and deduplicating, the obtained genes were normalized into the official symbol format using UniProt (http://www.uniprot.org/, accessed on June 17, 2025)[27]. Drug targets for osimertinib were finally obtained.

**Gene Ontology (GO) and Kyoto Encyclopedia of Genes and Genomes (KEGG) enrichment analysis**

To investigate the functions of co-expressed genes associated with cardiotoxicity and pulmotoxicity, GO and KEGG enrichment analysis were performed using the R clusterProfiler package (version 4.4.1)[28]. According to the P value < 0.05 and p.adjust <0.05, the top 10 significantly enriched terms in biological process (BP), molecular function (MF), cellular component (CC), along with the top 30 KEGG pathways (top 10 in bar chart, top 20 in Sankey bubble chart), were selected for visualization.

For the functional analysis of osimertinib in cardio-pulmotoxicity, intersecting targets underwent

further GO and KEGG analyses. All the GO results and the KEGG results were displayed by the SRplot platform (https://www.bioinformatics.com.cn, accessed on June 19, 2025) [29] for data analysis and visualization.

**Construction of a disease-target-pathway network**

An integrated network illustrating the interactions among osimertinib, shared targets, and the top 10 enriched GO terms and KEGG pathways was constructed using Cytoscape software (Version 3.7.0).

**Construction of the Protein-Protein Interaction (PPI) network**

The PPI networks associated with osimertinib-cardiotoxicity-pulmotoxicity in the human genome were constructed by the String database (Version 12.0) (https://string-db.org/, accessed on June 20, 2025). All searches were employed with the species parameter restricted to *Homo sapiens* and filtered to include only interactions with a high confidence score of 0.9 or greater[30]. After hiding the discrete network node, a TSV format file was downloaded and subsequently imported into Cytoscape (version 3.7.0) for further analysis.

**Identification of hub genes**

The PPI network was imported into the Cytoscape (version 3.7.0) for further analysis. The Molecular Complex Detection (MCODE) algorithm [31] for analysis with the criterion set as follows: k-core = 2, node score cut-off = 0.2, degree cutoff = 2, and maximum depth =100. Subsequently, four algorithms[32]: Degree, Edge Percolation Component (EPC), Maximum Cluster Centrality (MCC), and Maximum Neighborhood Component (MNC), were used in the CytoHubba plugin to calculate scores and identify the top 10 hub genes. The final hub genes were determined by the intersection of the results from the four algorithms.

**Verification of osimertinib-targets binding via molecular docking**

Molecular docking analysis was used to clarify the above results further. Osimertinib was chosen and docked with the final seven hub gene targets in the PPI network. The 3D structure of osimertinib was downloaded from the PubChem database (https://pubchem.ncbi.nlm.nih.gov/, accessed on June 27, 2025) and saved as an SDF format file. The target structures were downloaded from the Protein Data Bank database (PDB, https://www.rcsb.org/, accessed on June 27, 2025) and imported into the Pymol Software 2.6 for removing solvent and organic. Then, the 3D structure of osimertinib and the target crystal structure were subsequently converted into a pdbqt format file, and the docking grid box of each target protein was constructed by AutoDockTools 4.2. The molecular docking process between

osimertinib and each target protein was carried out by AutoDock Vina 1.2.6 software. The conformation with the lowest calculated binding energy (BE) was selected, and docking images were visualized using Pymol 2.6 and Discovery Studio 2021.

**Verification of the binding model using MDS**

The GROMACS 2022.3 package [34] was utilized to carry out the MDS. The protein was simulated with the AMBER99SB-ILDN force field. The small molecule was parameterized using the GAFF2 force field, and its geometry was optimizede B3LYP/6-31G(d) level with Gaussian 16W. RESP charges were fitted with Multiwfn. Subsequently, the simulation system was prepared by placing the complex within a cubic periodic box with a minimum of 1.0 nm distance between the surface of the complex and the edge of the box. The system was then solvated under the TIP3P water model and neutralized with the addition of 0.15 M NaCl. At 310 K and 1 bar, thermodynamic stability of the system was maintained using the velocity-rescale thermostat (coupling time constant 0.1 ps) and Parrinello-Rahman barostat (coupling time constant 2.0 ps). Simulation protocol began with energy minimization employing the steepest descent algorithm, with two equilibration steps: a 100 ps NVT ensemble simulation with restraints on the protein backbone to gradually raise the system temperature to 310 K, and a 100 ps NPT ensemble simulation with no restraints to equilibrate the system density to 1.0±0.02 g/cm³ (trajectories every 100 ps were saved for monitoring). Finally, an unconstrained 100 ns production simulation was performed with a time step of 2 fs, and one frame was saved every 10 ps. Root mean square deviation (RMSD), radius of gyration (Rg), root mean square fluctuation (RMSF), hydrogen bond (HB), and solvent accessible surface area (SASA) were calculated for trajectory analysis. The free energy landscape (FEL) was also constructed based on the principal component analysis (PCA) data. Following the completion of MDS, molecular mechanics Poisson-Boltzmann surface area (MMPBSA) was utilized to calculate the average binding free energies of the target complexes systematically. A residue-level energy decomposition analysis was performed and visualized using Origin 2021.

## Results

**Landscape of genes co-expressed in cardiotoxicity and pulmotoxicity**

Potential target genes associated with cardiotoxicity and pulmotoxicity were identified using GeneCards, OMIM, and TTD databases, respectively. After combining and eliminating duplicated genes, A total of 5923 genes associated with cardiotoxicity (Fig. 2A, Supplementary Table S1) and

3827 genes related to pulmotoxicity were identified (Fig. 2B, Supplementary Table S2). Venn diagrams showed that the intersection of 3043 genes was associated with both cardio-pulmotoxicity (Fig. 2C, Supplementary Table S3). To explore the signaling pathway and functions of predicted targets, the above intersection of 3043 genes was further analyzed using the Bioconductor platform for GO and KEGG enrichment analysis. A total of 6882 GO-enriched items were obtained, including 5633 BP terms, 797 MF terms, and 452 CC terms (Supplementary Table S4). According to the P-value, the top 10 GO enrichment items were visualized via a bar diagram (Fig. 2D). Notably, the most significantly enriched BP term was "morphogenesis of an epithelium", while significant enrichment in the CC category was seen in "collagen-containing extracellular matrix" and in "DNA-binding transcription factor binding" in MF. A total of 210 KEGG-enriched items were obtained (Supplementary Table S5), and the top 30 KEGG-enriched items were visualized via a bar diagram (Fig. 2E). The most significant KEGG pathway was "PI3K-Akt signaling pathway".

**Network pharmacology analysis of potential target genes common to both osimertinib and cardio-pulmotoxicity**

The 2D and 3D structures of osimertinib were illustrated in Fig. 3A. Potential osimertinib genes were identified using the ChEMBL, STITCH, and SwissTargetPrediction databases, respectively. After combining and eliminating duplicated genes, a total of 356 potential osimertinib targets were identified (Fig. 3B, Supplementary Table S6). Venn diagrams identified 119 potential target genes common to both osimertinib and cardio-pulmotoxicity (Fig. 3C, Supplementary Table S7). These genes were associated with 4096 biological pathways, including 3996 GO (Supplementary Table S8) and 100 KEGG pathways (Supplementary Table S9). GO analysis identified 3358 terms in BP, 220 in CC, and 418 in MF. According to the P-value, the top 10 GO enrichment items were visualized via a bar diagram (Fig. 3D). The chord diagram and bubble diagram were used to visualize the top 5 enriched terms in the BP, CC, and MF categories (Fig. 3D). In BP terms, it primarily involves epigenetic regulation of gene expression (GO: 0040029, n=28), response to xenobiotic stimulus (GO:0009410, n=23), rhythmic process (GO:0048511, n=23), negative regulation of gene expression, epigenetic (GO:0045814, n=22), heterochromatin formation (GO:0031507, n=19). MF enrichment mainly includes histone modifying activity (GO: 0140993, n=38), DNA-binding transcription factor binding (GO: 0140993, n=29), RNA polymerase II-specific DNA-binding transcription factor binding (GO:0061629, n=23), transcription coactivator activity (GO:0003713, n=18), transcription corepressor

activity (GO:0003714, n=16). In CC terms, it primarily involves the methyltransferase complex (GO: 0034708, n=12). The top 10 and 20 KEGG top enrichment items were visualized via a bar diagram and Sankey bubble chart, respectively (Fig. 3E). Osimertinib and cardio-pulmotoxicity targets primarily involve MicroRNAs in cancer (hsa05206, n=21), viral carcinogenesis (hsa05203, n=20), thyroid hormone signaling pathway (hsa04919, n=19), PI3K-Akt signaling pathway (hsa04151, n=18), and human papillomavirus infection (hsa05165, n=17). A Disease-Drug-Targets-Pathways interaction network based on the common targets, the top 10 BP, 10 CC, 10 MF, and the top 10 KEGG pathways was constructed and visualized using Cytoscape (Fig. 3F). The result reflected that the mechanism of osimertinib and cardio-pulmotoxicity was based on multiple targets and multiple pathways working synergistically.

**Identification of hub genes between osimertinib and cardio-pulmotoxicity**

The intersection targets related to osimertinib and cardio-pulmotoxicity were imported into the String database, which was performed with the term "*Homo sapiens*", and were filtered with the highest confidence score of 0.9 or greater. The PPI network was first built with 87 nodes (hide disconnected nodes in the network) and 286 edges. Then it was visualized via Cytoscape with 84 nodes (SCN5A, KCHN2, PDE5A, and PDE2A were hidden) and 284 edges (Fig. 4A). Functional analysis using the MCODE plugin identified highly interconnected gene clusters, leading to the identification of the top 13 hub genes and 35 edges (Fig. 4B). The top 10 hub genes were then identified using the CytoHubba plugin with the"Degree, EPC, MCC, and MNC" algorithms (Fig. 4C). An UpSet plot demonstrated that seven hub genes were consistently identified by all four algorithms (Fig. 4D). These targets were TP53 (tumor protein P53), ESR1 (estrogen receptor alpha 1), HDAC1 (Histone Deacetylase1), CREBBP (CREB binding protein), EP300 (E1A binding protein p300), HDAC2 (Histone Deacetylase2), and SMARCA4 (SWI/SNF-related matrix-associated actin-dependent regulator of chromatin subfamily A member 4).

**Verification of interactions between osimertinib and potential targets through molecular docking**

Structures of receptor proteins were obtained from the PDB database: TP53 (1UOL), ESR1 (4ZN7), HDAC1 (4BKX), CREBBP (5EP7), EP300 (3I3J), HDAC2 (4LY1), and SMARCA4 (2GRC). The molecular docking process between osimertinib and each target protein was carried out using Autodock Vina 1.2.6 software, and the result of the lowest calculated binding energy (BE) was selected. Docking images were visualized using Discovery Studio 2021. As shown in Fig. 5, osimertinib bound with high

affinity to all seven genes, with the following docking scores: TP53, -6.7 kcal/mol; HDAC2, -6.9 kcal/mol; HDAC1, -7.6 kcal/mol; ESR1, -6.4 kcal/mol; EP300, -6.9 kcal/mol; CREBBP, -7.2 kcal/mol; SMARCA4, -6.5 kcal/mol. As shown in Fig. 5, all seven binding energies were more negative than −6.0 kcal/mol, indicating stable binding (Fig. 5). Of them, the binding energies of the osimertinib-HDAC1 and osimertinib-CREBBP complexes were the lowest, with the best binding stability. 3D structural analysis showed that osimertinib formed four hydrogen bonds with HDAC1 through the amino acid residues ASN-307, GLY-268, ARG-310, and HIS-344, respectively. Osimertinib formed two hydrogen bonds with CREBBP through the amino acid residues TYR-1167 and ASN-1168, respectively.

**Verification of binding capacity through MDS**

Based on their lowest binding energies, HDAC1 and CREBBP were selected for subsequent MDS validation. RMSD and RMSF showed that the osimertinib and HDAC1, CREBBP complexes both stabilized after 10 ns simulation, with stable osimertinib binding at the active sites without significant displacement (Fig. 6A, B). RMSF analysis identifiedseveral high-flexibility zones in the osimertinib-HDAC1 complex, specifically residues 200-225, where RMSF values were approximately 0.7 nm. The osimertinib-CREBBP complex also exhibited evident peaks around residue 1060, residue 1120, and residue 1170 (Fig. 6B). These results indicated higher flexibility regions that may be similar to significant binding sites for osimertinib. The results of Rg and SASA revealed that both osimertinib-HDAC1 and osimertinib-CREBBP complexes preferred more compact folding conformations upon osimertinib binding, suggesting increased structural stability (Fig. 6C, D). Analysis of HB revealed the occurrence of five and four stable hydrogen bonds in the osimertinib-HDAC1 and osimertinib-CREBBP complexes, respectively, which significantly contributed to complex stabilization (Fig. 6E). The 2D and 3D representations of the Gibbs free energy between osimertinib and HDAC1, CREBBP were presented in Fig. 7A, B. The binding free energy values were -20.85 kcal/mol for osimertinib-HDAC1 and -22.92 kcal/mol for osimertinib-CREBBP in the 100 ns simulation time, indicating strong and stable binding (Fig. 7C). Strikingly, the osimertinib-CREBBP complex had the most stable binding orientation since it was the optimal binding free energy. Energy decomposition analysis identified significant residues contributing substantially to the binding interaction, ILE-345, ARG-310, and LYS-342 for HDAC1, and ILE-1122, VAL-1174, and VAL-1115 for CREBBP (Fig. 7D). These findings in total constitute robust evidence that osimertinib was stably bound to HDAC1 and

CREBBP in MDS, and that such interactions were likely to play significant biological roles in mediating the pharmacology and toxicity of osimertinib. The workflow is illustrated in Fig. 1.

**Discussion**

Although the effectiveness of osimertinib as a treatment in EGFR T790M-mutant NSCLC was shown, its cardiotoxicity[13] and pulmotoxicity[17] partially limited its clinical application, and pathways of molecular regulation of such toxicities remain not fully elucidated. To address this unresolved scientific question, the present work constructed a computational pharmacology strategy integrating network toxicology, molecular docking, and MDS to methodically disentangle the potential molecular mechanisms by which osimertinib induced dual-organ toxicity in the lung and heart. Our analysis indicated that osimertinib-induced cardio-pulmotoxicity may originate from its systemic disruption of a complex epigenetic regulatory network. This network centered on the histone acetyltransferases CREBBP/EP300 and histone deacetylases HDAC1/HDAC2, and engaged in functional crosstalk with key regulators such as TP53, ESR1, and SMARCA4. The finding provided a novel theoretical framework for understanding the molecular mechanism of osimertinib and cardio-pulmotoxicity and served as a foundation for follow-up research.

Our study discovered that osimertinib-induced cardio-pulmotoxicity was closely associated with its functional inhibition of histone acetyltransferases CREBBP and EP300. MDS indicated that CREBBP might be the most important target with the lowest binding free energy with osimertinib, suggesting a significant interaction between them. These two transcriptional coactivators with high structural and functional homology[33] constitute a core component of the epigenetic regulation network. CREBBP in lung tissue acts as a key node in the competitive endogenous RNA network, finely regulating the balance of gene expression of lung cancer-related genes[34]. In the heart, CREBBP is involved in inflammation and fibrosis coupled with sphingolipid metabolism[35], whereas EP300 protects endothelial function and mitochondrial homeostasis by modulating signaling pathways such as JAK/STAT[36]. Notably, CREBBP/EP300 is frequently mutated in numerous cancers, which not only enhances tumor development[37] but also is significantly associated with decreased relapse-free survival of small cell lung cancer patients after chemotherapy[38]. Additionally, EP300 enhances endothelial dysfunction by regulating histone acetylation of the SOCS1 promoter region in the cardiovascular system[36] while it plays oncogenic roles during the development of lung cancer via the Hippo-YAP[39] and Wnt[40] signaling pathways. Based on these findings, we speculated that

osimertinib would disrupt the shared epigenetic regulatory node of CREBBP/EP300, leading to homeostatic imbalance in different organ systems, including the heart and lung.

In addition to the roles of CREBBP and EP300, our study also indicated the function of HDAC1 and HDAC2 in osimertinib-induced cardio-pulmotoxicity. In the cardiac system, HDAC1 and HDAC2 both play a role in pathological cardiac remodeling regulation, and both exhibit increased expression in models of heart failure[41, 42]. Studies have shown that inhibition of HDAC1 enhances cardiac remodeling following myocardial infarction by inhibiting cardiomyocyte apoptosis[43], whereas HDAC2 controls ventricular electrical remodeling in the early stage of heart failure by adjusting the function of ion channels[44]. Remarkably, inhibition of both HDAC1 and HDAC2 at the same time corrects interstitial fibrosis to a significant extent in chronic heart failure[42], suggesting functional cooperation between these two epigenetic regulators in cardiac pathological processes. HDAC1 is involved in lung cancer pathogenesis in terms of its site-specific phosphorylation modifications[45], while HDAC2 regulates airway inflammation and tissue repair by inhibiting IL-17A[46, 47]. Importantly, studies show that the expression of HDAC2 and HDAC3 synergizeinhibitor therapy in NSCLC [48] and that activation of the HDAC1/JAK1/FGL1 pathway boosts anti-cancer immune responses[49]. Based on these data, we reasoned that osimertinib might disrupt the homeostatic balance of cardiopulmonary tissue by virtue of concurrent interference with HDAC1 and HDAC2, an epigenetically synergistic deacetylase pair.

CREBBP/EP300 and HDAC1/HDAC2 form an epigenetically balanced dynamic regulatory axis, collectively maintaining gene expression homeostasis of cardiopulmonary tissues. Simultaneously, TP53, SMARCA4, and ESR1 were crucial regulating elements playing pivotal roles in osimertinib-induced cardio-pulmotoxicity. TP53 modifies cardiac energy metabolism by regulating TIGAR[50] and minimizes drug-induced cardiac injury by maintaining mitochondrial DNA stability[51]. In lung disease, upregulated TP53 expression is implicated in the regulation of inflammation in chronic obstructive pulmonary disease, pointing to its important role in resistance of lung tissue to stress[52]. As a core component of chromatin remodeling complexes, SMARCA4 contributes to the development of pulmonary fibrosis through regulation of type II alveolar cell proliferation[53] and plays a critical role in lung injury repair. In cardiovascular diseases, SMARCA4 coordinates repair responses after myocardial damage to ensure cardiac structural integrity. ESR1 demonstrates significant clinical significance in both cardiovascular diseases and lung cancer. Evidence

suggests that ESR1 is an independent good prognostic predictor of survival for early-stage NSCLC patients[54]. In contrast, ESR1-AKAP12 gene fusions can induce osimertinib resistance[55], while its mRNA expression level is a predictive factor for patient survival status[56]. Cardiovascularly, ESR1 gene variants significantly increase the risk of coronary heart disease in men by promoting the progression of atherosclerosis [57]. These are key factors, besides the CREBBP/EP300 and HDAC1/HDAC2 epigenetic regulatory pathway, that contribute to a multi-layered regulatory system generating synergistic effects in osimertinib-induced cardio-pulmotoxicity, that collectively control disease onset and progression.

GO enrichment results indicated that these targets were primarily involved in epigenetic regulation mechanisms. Specifically, they were enriched in BP terms of “epigenetic regulation of gene expression” and “heterochromatin formation”, MF term of “histone modifying activity”, and CC term of “methyltransferase complex”. These findings are consistent with the known functions of several core targets, including CREBBP, EP300, HDAC1, HDAC2, and SMARCA4. Notably, KEGG pathway analysis revealed significant enrichment in cancer-related pathways. The most significant enrichment in “MicroRNAs in cancer” pathways further substantiates the interconnectedness among these targets. Research has demonstrated that microRNAs can regulate the expression of multiple core genes, including EP300[58], TP53[59], and HDAC1[60], thereby establishing a complex regulatory network that may amplify the toxic effects of osimertinib. Furthermore, the “PI3K-Akt signaling pathway” emerged as a central pathway connecting multiple core targets. Previous studies have confirmed that TP53[61], HDAC1[62], and CREBBP[63] are all associated with the PI3K-Akt pathway. These functional enrichment results supported our hypothesis that osimertinib-induced cardio-pulmotoxicity occurred through simultaneous disruption of multiple epigenetic regulators and signaling pathways.

Although this study systematically untangled the potential molecular mechanisms of osimertinib-induced cardio-pulmotoxicity by integrating network toxicology, molecular docking, and MDS, several limitations remain. First, the findings are primarily based on computational predictions and require experimental validation. Although molecular docking and MDS provided strong theoretical support for the interactions between osimertinib and core targets, these predictions need to be further confirmed in cellular and animal models. Second, the study did not fully elucidate the causal relationships between epigenetic regulation and signaling pathways. Although significant enrichment was observed in pathways such as PI3K-Akt, the specific regulatory relationships between these

pathways and epigenetic regulators warrant further investigation. Despite these limitations, this study provided a theoretical framework and experimental directions for understanding the toxic side effects of osimertinib. Subsequent research will validate the core findings in vivo and in vitro experiments.

## Conclusion

In summary, our integrated analysis identified TP53, ESR1, HDAC1, CREBBP, EP300, HDAC2, and SMARCA4 as core targets, and HDAC1 and CREBBP as potential core hubs in the toxicity mechanism. Multiple pathways, most significantly the MicroRNAs in cancer signaling pathway, were implicated in the process. Taken together, these findings support the hypothesis that: osimertinib induces cardio-pulmotoxicity by disrupting epigenetic balance between CREBBP/EP300 and HDAC1/HDAC2, in addition to engaging in multi-target interactions with TP53, ESR1, and SMARCA4. This work thereby outlines a multi-target, epigenetics-centered fra

mework that may guide future experimental validation of osimertinib-mediated toxicity.

## References


[1] Ricotti A, Sciannameo V: Incidence and Prevalence Analysis of Non-Small-Cell and Small-Cell Lung Cancer Using Administrative Data. Int J Environ Res Public Health 2021, 18(17):9076. https://doi.org/10.3390/ijerph18179076

[2] Alduais Y, Zhang H, Fan F, Chen J: Non-small cell lung cancer (NSCLC): A review of risk factors, diagnosis, and treatment. Medicine (Baltimore) 2023, 102(8):e32899. https://doi.org/10.1097/md.0000000000032899

[3] Diseases GAoT: Consensus on Postoperative Recurrence Prediction of Non-small Cell Lung Cancer Based on Molecular Markers. Zhongguo Fei Ai Za Zhi 2022, 25(10):701-714. https://doi.org/10.3779/j.issn.1009-3419.2022.102.44

[4] Pao W, Chmielecki J: Rational, biologically based treatment of EGFR-mutant non-small-cell lung cancer. Nat Rev Cancer 2010, 10(11):760-774. https://doi.org/10.1038/nrc2947

[5] Hatat AS, Benoit-Pilven C, Pucciarelli A, de Fraipont F, Lamothe L, Perron P, Rey A, Levra MG, Toffart AC, Auboeuf D et al: Altered splicing of ATG16-L1 mediates acquired resistance to tyrosine kinase inhibitors of EGFR by blocking autophagy in non-small cell lung cancer. Mol Oncol 2022, 16(19):3490-3508. https://doi.org/10.1002/1878-0261.13229

[6] Castellanos EH, Horn L: Generations of Epidermal Growth Factor Receptor Tyrosine Kinase Inhibitors: Perils and Progress. Curr Treat Options Oncol 2015, 16(10):51. https://doi.org/10.1007/s11864-015-0365-1

[7] Matsumoto Y, Kawaguchi T, Watanabe M, Isa SI, Ando M, Tamiya A, Kubo A, Kitagawa C,

Yoshimoto N, Koh Y: Prognostic impact of pretreatment T790M mutation on outcomes for patients with resected, EGFR-mutated, non-small cell lung cancer. BMC cancer 2022, 22(1):775. https://doi.org/10.1186/s12885-022-09869-7

[8] Song X, Cao L, Ni B, Wang J, Qin X, Sun X, Xu B, Wang X, Li J: Challenges of EGFR-TKIs in NSCLC and the potential role of herbs and active compounds: From mechanism to clinical practice. Frontiers in pharmacology 2023, 14:1090500. https://doi.org/10.3389/fphar.2023.1090500

[9] Gilardone S, Thapa R, Laborde J, Shafique M, Saltos A, Creelan B, Tanvetyanon T, Chiappori A, Simon G, Haura EB et al: Osimertinib vs. afatinib as first-line treatment for patients with metastatic non-small cell lung cancer with an EGFR exon 19 deletion or exon 21 L858R mutation. J Thorac Dis 2023, 15(11):6115-6125. https://doi.org/10.21037/jtd-23-686

[10] Kuo JS, Chang CY, Chang SC: Rebiopsy Enhances Survival with Afatinib vs. Osimertinib in EGFR Exon 19 Deletion Non-Small Cell Lung Cancer: A Multicenter Study in Taiwan. Curr Oncol 2025, 32(1):36. https://doi.org/10.3390/curroncol32010036

[11] Greig SL: Osimertinib: First Global Approval. Drugs 2016, 76(2):263-273. https://doi.org/10.1007/s40265-015-0533-4

[12] Barbieri MA, Sorbara EE, Cicala G, Santoro V, Cutroneo PM, Franchina T, Santarpia M, Silvestris N, Spina E: Safety profile of tyrosine kinase inhibitors used in non-small-cell lung cancer: An analysis from the Italian pharmacovigilance database. Frontiers in oncology 2022, 12:1005626. https://doi.org/10.3389/fonc.2022.1005626

[13] Waliany S, Zhu H, Wakelee H, Padda SK, Das M, Ramchandran K, Myall NJ, Chen T, Witteles RM, Neal JW: Pharmacovigilance Analysis of Cardiac Toxicities Associated With Targeted Therapies for Metastatic NSCLC. J Thorac Oncol 2021, 16(12):2029-2039. https://doi.org/10.1016/j.jtho.2021.07.030

[14] Ewer MS, Tekumalla SH, Walding A, Atuah KN: Cardiac Safety of Osimertinib: A Review of Data. J Clin Oncol 2021, 39(4):328-337. https://doi.org/10.1200/jco.20.01171

[15] Bak M, Park H, Lee SH, Lee N, Ahn MJ, Ahn JS, Jung HA, Park S, Cho J, Kim J et al: The Risk and Reversibility of Osimertinib-Related Cardiotoxicity in a Real-World Population. J Thorac Oncol 2025, 20(2):167-176. https://doi.org/10.1016/j.jtho.2024.10.003

[16] Yu HY, Lee CY, Hu YC, Lin LG, Chao Y, Li CP: Treatment rechallenge is safe and leads to better survival in pancreatic cancer patients with interstitial pneumonitis. BMC cancer 2025, 25(1):508. https://doi.org/10.1186/s12885-025-13896-5

[17] Kobayashi T, Watanabe K: Clinical outcomes of patients with EGFR-mutated NSCLC developing interstitial lung disease during first-line osimertinib therapy: a sub-analysis of the Reiwa study. Jpn J Clin Oncol 2025, 55(3):275-282. https://doi.org/10.1093/jjco/hyae178

[18] Sato Y, Sumikawa H, Shibaki R, Morimoto T, Sakata Y, Oya Y, Tamiya M, Suzuki H, Matsumoto H, Yokoi T et al: Drug-Related Pneumonitis Induced by Osimertinib as First-Line Treatment for Epidermal Growth Factor Receptor Mutation-Positive Non-Small Cell Lung Cancer: A Real-World Setting. Chest 2022, 162(5):1188-1198. https://doi.org/10.1016/j.chest.2022.05.035

[19] Zou T, Zhang R, Hu L, Yang G, Chen X, Wang M, Cheng T, Nie S, Liu L, Hong S: Uncovering mechanism of hepatotoxicity diseases caused by tetrahydrocannabinol based on novel network toxicology and experimental verification. Sci Rep 2025, 15(1):13712. https://doi.org/10.1038/s41598-025-97523-0

[20] Chen Q, Zhang K, Jiao M, Jiao J, Chen D, Yin Y, Zhang J, Li F: Study on the Mechanism of Mesaconitine-Induced Hepatotoxicity in Rats Based on Metabonomics and Toxicology Network. Toxins 2022, 14(7):486. https://doi.org/10.3390/toxins14070486

[21] Sun J, Liu X, Zhao S, Zhang S, Yang L, Zhang J, Zhao M, Xu Y: Prediction and verification of potential lead analgesic and antiarrhythmic components in Corydalis yanhusuo W. T. Wang based on voltage-gated sodium channel proteins. Int J Biol Macromol 2022, 216:537-546. https://doi.org/10.1016/j.ijbiomac.2022.07.024

[22] Amberger JS, Bocchini CA, Scott AF, Hamosh A: OMIM.org: leveraging knowledge across phenotype-gene relationships. Nucleic Acids Res 2019, 47:D1038-D1043. https://doi.org/10.1093/nar/gky1151

[23] Zhou Y, Zhang Y, Zhao D, Yu X, Shen X, Zhou Y, Wang S, Qiu Y, Chen Y, Zhu F: TTD: Therapeutic Target Database describing target druggability information. Nucleic Acids Res 2024, 52(D1):D1465-D1477. https://doi.org/10.1093/nar/gkad751

[24] Zdrazil B, Felix E, Hunter F, Manners EJ, Blackshaw J, Corbett S, de Veij M, Ioannidis H, Lopez DM, Mosquera JF et al: The ChEMBL Database in 2023: a drug discovery platform spanning multiple bioactivity data types and time periods. Nucleic Acids Res 2024, 52(D1):D1180-D1192. https://doi.org/10.1093/nar/gkad1004

[25] Daina A, Michielin O, Zoete V: SwissTargetPrediction: updated data and new features for efficient prediction of protein targets of small molecules. Nucleic Acids Res 2019, 47(1362-4962 (Electronic)):W357-W364. https://doi.org/10.1093/nar/gkz382

[26] Xi YA-O, Zhao T, Shi M, Zhang X, Bao Y, Gao J, Shen J, Wang H, Xie Z, Wang QA-O et al: Potential Therapeutic Mechanism of Radix Angelicae Biseratae and Dipsaci Radix Herb Pair against Osteoarthritis: Based on Network Pharmacology and Molecular Docking. Evid Based Complement Alternat Med 2023:2140327. https://doi.org/10.1155/2023/2140327

[27] Consortium U: UniProt: the Universal Protein Knowledgebase in 2023. Nucleic Acids Res 2023, 51(1362-4962 (Electronic)):D523-D531. https://doi.org/10.1093/nar/gkac1052

[28] Yu G, Wang Lg Fau - Han Y, Han Y Fau - He Q-Y, He QY: clusterProfiler: an R package for comparing biological themes among gene clusters. OMICS 2012, 16(1557-8100 (Electronic)):284-287. https://doi.org/10.1089/omi.2011.0118

[29] Tang D, Chen M, Huang X, Zhang G, Zeng L, Zhang G, Wu S, Wang YA-O: SRplot: A free online platform for data visualization and graphing. PLoS One 2023, 18(1932-6203 (Electronic)):e0294236. https://doi.org/10.1371/journal.pone.0294236

[30] Yadav RP, Sadhukhan S, Saha ML, Ghosh S, Das M: Exploring the mechanism of andrographolide in the treatment of gastric cancer through network pharmacology and molecular docking. Sci Rep 2022, 12(1):18413. https://doi.org/10.1038/s41598-022-18319-0

[31] Bader GD, Hogue CW: An automated method for finding molecular complexes in large protein interaction networks. BMC bioinformatics 2003, 4:2. https://doi.org/10.1186/1471-2105-4-2

[32] Li J, Yan X, Li B, Huang L, Wang X, He B, Xie H, Wu Q, Chen L: Identification and validation of ferroptosis-related genes in patients infected with dengue virus: implication in the pathogenesis of DENV. Virus genes 2023, 59(3):377-390. https://doi.org/10.1007/s11262-023-01985-1

[33] Cui G, Ley M, Mechaly AE, Bui LC, Michail C, Berthelet J, Dairou J, Yang H, Chevreux G, Moroy G et al: Structural and functional characterization of CREB-binding protein (CREBBP)

as a histone propionyltransferase. J Biol Chem 2025, 301(8):110444. https://doi.org/10.1016/j.jbc.2025.110444

[34] Wang Y, Fu Y: Identification of circRNA-miRNA-mRNA networks to explore underlying mechanism in lung cancer. Health Inf Sci Syst 2025, 13(1):5. https://doi.org/10.1007/s13755-024-00318-2

[35] Qu Y, Ma D, Wu T, Wang H, Tian Z, Liu X, Wang Y: A multi-omics approach identifies the key role of disorders of sphingolipid metabolism in Ang II-induced hypertensive cardiomyopathy myocardial remodeling. Sci Rep 2024, 14(1):30379. https://doi.org/10.1038/s41598-024-81611-8

[36] Xue W, Deng L: EP300 improves endothelial injury and mitochondrial dysfunction in coronary artery disease by regulating histone acetylation of SOCS1 promoter via inhibiting JAK/STAT pathway. Cytokine 2024, 176:156507. https://doi.org/10.1016/j.cyto.2024.156507

[37] Wu Z, Wu H, Dai Y, Wang Z, Han H, Shen Y, Zhang R, Wang X: A pan-cancer multi-omics analysis of lactylation genes associated with tumor microenvironment and cancer development. Heliyon 2024, 10(5):e27465. https://doi.org/10.1016/j.heliyon.2024.e27465

[38] George J, Maas L: Evolutionary trajectories of small cell lung cancer under therapy. Nature 2024, 627(8005):880-889. https://doi.org/10.1038/s41586-024-07177-7

[39] Li S, Shi J, Wang L, Zhang D, Zhang H: EP300 promotes lung cancer cell proliferation by regulating the oncogenic transcription of Hippo-YAP signaling pathway. Biochem Biophys Res Commun 2024, 692:149330. https://doi.org/10.1016/j.bbrc.2023.149330

[40] Sun Y, Sun J, Ying K, Chen J, Chen T, Tao L, Bian W, Qiu L: EP300 regulates the SLC16A1-AS1-AS1/TCF3 axis to promote lung cancer malignancies through the Wnt signaling pathway. Heliyon 2024, 10(6):e27727. https://doi.org/10.1016/j.heliyon.2024.e27727

[41] Montgomery RL, Davis CA, Potthoff MJ, Haberland M, Fielitz J, Qi X, Hill JA, Richardson JA, Olson EN: Histone deacetylases 1 and 2 redundantly regulate cardiac morphogenesis, growth, and contractility. Genes & development 2007, 21(14):1790-1802. https://doi.org/10.1101/gad.1563807

[42] Nural-Guvener HF, Zakharova L, Nimlos J, Popovic S, Mastroeni D, Gaballa MA: HDAC class I inhibitor, Mocetinostat, reverses cardiac fibrosis in heart failure and diminishes CD90+ cardiac myofibroblast activation. Fibrogenesis & tissue repair 2014, 7:10. https://doi.org/10.1186/1755-1536-7-10

[43] Wang L, Du A, Lu Y, Zhao Y, Qiu M, Su Z, Shu H, Shen H, Sun W, Kong X: Peptidase Inhibitor 16 Attenuates Left Ventricular Injury and Remodeling After Myocardial Infarction by Inhibiting the HDAC1-Wnt3a-β-Catenin Signaling Axis. J Am Heart Assoc 2023, 12(10):e028866. https://doi.org/10.1161/jaha.122.028866

[44] Syren P, Rahm AK, Schweizer PA, Bruehl C, Katus HA, Frey N, Thomas D, Lugenbiel P: Histone deacetylase 2-dependent ventricular electrical remodeling in a porcine model of early heart failure. Life sciences 2021, 281:119769. https://doi.org/10.1016/j.lfs.2021.119769

[45] Cai M, Xiao Y, Zheng J, Shi J, Wu J, Kong X, Liang Z: Mapping Context-Aware Phosphosite Regulation of Protein-Protein Interactions Using Deep Learning and Pan-Cancer Proteomics. J Chem Inf Model 2025, 65(20):11255-11271. https://doi.org/10.1021/acs.jcim.5c01504

[46] Ouyang L, Su G, Quan J, Xiong Z, Lai T: Emerging roles and therapeutic implications of HDAC2 and IL-17A in steroid-resistant asthma. Chin Med J Pulm Crit Care Med 2023,

1(2):108-112. https://doi.org/10.1016/j.pccm.2023.04.003

[47] Lai T, Tian B, Cao C, Hu Y, Zhou J, Wang Y, Wu Y, Li Z, Xu X, Zhang M et al: HDAC2 Suppresses IL17A-Mediated Airway Remodeling in Human and Experimental Modeling of COPD. Chest 2018, 153(4):863-875. https://doi.org/10.1016/j.chest.2017.10.031

[48] Booth L, West C, Moore RP, Von Hoff D, Dent P: GZ17-6.02 and Pemetrexed Interact to Kill Osimertinib-Resistant NSCLC Cells That Express Mutant ERBB1 Proteins. Frontiers in oncology 2021, 11:711043. https://doi.org/10.3389/fonc.2021.711043

[49] Xu T, Fang Y, Gu Y, Xu D, Hu T, Yu T, Xu YY, Shen HY, Ma P, Shu Y: HDAC inhibitor SAHA enhances antitumor immunity via the HDAC1/JAK1/FGL1 axis in lung adenocarcinoma. J Immunother Cancer 2024, 12(10):e010077. https://doi.org/10.1136/jitc-2024-010077

[50] Okawa Y, Hoshino A, Ariyoshi M, Kaimoto S, Tateishi S, Ono K, Uchihashi M, Iwai-Kanai E, Matoba S: Ablation of cardiac TIGAR preserves myocardial energetics and cardiac function in the pressure overload heart failure model. Am J Physiol Heart Circ Physiol 2019, 316(6):H1366-h1377. https://doi.org/10.1152/ajpheart.00395.2018

[51] Nishi M, Wang PY, Hwang PM: Protective role of p53 in doxorubicin-induced cardiomyopathy as a mitochondrial disease. Molecular & cellular oncology 2020, 7(3):1724598. https://doi.org/10.1080/23723556.2020.1724598

[52] Sergio LPS, Lucinda LMF, Reboredo MM, de Paoli F, Fonseca LMC, Pinheiro BV, Mencalha AL, Fonseca AS: Emphysema induced by elastase alters the mRNA relative levels from DNA repair genes in acute lung injury in response to sepsis induced by lipopolysaccharide administration in Wistar rats. Experimental lung research 2018, 44(2):79-88. https://doi.org/10.1080/01902148.2017.1422158

[53] Peng D, Si D, Zhang R, Liu J, Gou H, Xia Y, Tian D, Dai J, Yang K, Liu E et al: Deletion of SMARCA4 impairs alveolar epithelial type II cells proliferation and aggravates pulmonary fibrosis in mice. Genes & diseases 2017, 4(4):204-214. https://doi.org/10.1016/j.gendis.2017.10.001

[54] Brueckl WM, Al-Batran SE, Ficker JH, Claas S, Atmaca A, Hartmann A, Rieker RJ, Wirtz RM: Prognostic and predictive value of estrogen receptor 1 expression in completely resected non-small cell lung cancer. Int J Cancer 2013, 133(8):1825-1831. https://doi.org/10.1002/ijc.28209

[55] Roper N, Brown AL, Wei JS, Pack S, Trindade C, Kim C, Restifo O, Gao S, Sindiri S, Mehrabadi F et al: Clonal Evolution and Heterogeneity of Osimertinib Acquired Resistance Mechanisms in EGFR Mutant Lung Cancer. Cell Rep Med 2020, 1(1):100007. https://doi.org/10.1016/j.xcrm.2020.100007

[56] Li W, Tse LA, Wang F: Prognostic value of estrogen receptors mRNA expression in non-small cell lung cancer: A systematic review and meta-analysis. Steroids 2015, 104:129-136. https://doi.org/10.1016/j.steroids.2015.09.005

[57] Kunnas T, Silander K, Karvanen J, Valkeapää M, Salomaa V, Nikkari S: ESR1 genetic variants, haplotypes and the risk of coronary heart disease and ischemic stroke in the Finnish population: a prospective follow-up study. Atherosclerosis 2010, 211(1):200-202. https://doi.org/10.1016/j.atherosclerosis.2010.01.026

[58] Tan M, Shen L, Hou Y: Epigenetic modification of BDNF mediates neuropathic pain via miR-30a-3p/EP300 axis in CCI rats. Bioscience reports 2020, 40(11):BSR20194442.

https://doi.org/10.1042/bsr20194442
[59] Luo Z, Cui R, Tili E, Croce C: Friend or Foe: MicroRNAs in the p53 network. Cancer letters 2018, 419:96-102. https://doi.org/10.1016/j.canlet.2018.01.013
[60] Li Y, Zhang K, Mao W: Inhibition of miR-34a prevents endothelial cell apoptosis by directly targeting HDAC1 in the setting of atherosclerosis. Mol Med Rep 2018, 17(3):4645-4650. https://doi.org/10.3892/mmr.2018.8411
[61] Alvarado-Ortiz E, Ortiz-Sánchez E, Sarabia-Sánchez MA, de la Cruz-López KG, García-Carrancá A, Robles-Flores M: Mutant p53 gain-of-function stimulates canonical Wnt signaling via PI3K/AKT pathway in colon cancer. J Cell Commun Signal 2023, 17(4):1389-1403. https://doi.org/10.1007/s12079-023-00793-4
[62] Dong R, Zhang X, Liu Y, Zhao T, Sun Z, Liu P, Xiang Q, Xiong J, Du X, Yang X et al: Rutin alleviates EndMT by restoring autophagy through inhibiting HDAC1 via PI3K/AKT/mTOR pathway in diabetic kidney disease. Phytomedicine 2023, 112:154700. https://doi.org/10.1016/j.phymed.2023.154700
[63] Daragmeh J, Barriah W, Saad B, Zaid H: Analysis of PI3K pathway components in human cancers. Oncology letters 2016, 11(4):2913-2918. https://doi.org/10.3892/ol.2016.4309

**Data availability statement**

The original contributions presented in the study are included in the article/Supplementary material; further inquiries can be directed to the corresponding author.

**Author contributions**

HY: Data curation, Investigation, Validation, Writing - original draft. JS: Data curation, Investigation, Validation, Visualization. JH: Investigation, Methodology, Software, Formal Analysis. ET: Resources, Investigation, Writing - review & editing. JZ: Conceptualization, Supervision, Project administration, Funding acquisition, Methodology, Writing - original draft, Writing - review & editingion.

**Funding**

The authors declare that financial support was received for the research and/or publication of this article. Source of funding: The work of the authors is supported by the Social Development Science and Technology Project of Wenling City(2024S00157, 2026S00024, 2026S00059)

**Conflict of interest**

The authors declare that the research was conducted in the absence of any commercial or financial

relationships that could be construed as a potential conflict of interest.

**Generative AI statement**

The authors declare that no Generative AI was used in the creation of this manuscript.

**Fig. Legends**

Fig. 1 A flowchart of the network pharmacology analysis used in the study.

Fig. 2 Identification of targets associated with cardiotoxicity and pulmotoxicity. (A) Venn diagrams showing the number of targets associated with cardiotoxicity obtained from three different databases. (B) Venn diagrams showing the number of targets associated with pulmotoxicity obtained from three different databases. (C) Venn diagrams showing overlapping targets between cardiotoxicity and pulmotoxicity. (D) GO analysis of these overlapping 3043 targets. (E) KEGG pathway enrichment analysis of the overlapping targets. GO: Gene Ontology; KEGG: Kyoto Encyclopedia of Genes and Genomes.

Fig. 3 GO functional annotation and KEGG pathway enrichment of therapeutic targets for osimertinib and cardio-pulmotoxicity. (A) Structural formula of osimertinib from the PubChem database. (B) Integrated osimertinib targets derived from three drug databases. (C) Intersection between osimertinib targets and cardio-pulmotoxicity targets. (D) GO analysis of the 119 overlapping genes. (E) KEGG pathway analysis of the 119 overlapping genes. (F) Construction of the Disease-Drug-Targets-Pathways interaction network for the top 10 GO, top 10 KEGG pathways, and the overlapping genes. GO: Gene Ontology; KEGG: Kyoto Encyclopedia of Genes and Genomes.

Fig. 4Identification of hub genes using Cytoscape and the STRING database. (A) PPI network of 87 overlapping genes constructed via the STRING database and Cytoscape software. (B) Significant modules within the PPI network identified by the MCODE algorithm. (C) The top 10 genes with the highest connectivity in the PPI network were determined by Cytoscape (D) UpSet plot illustrating the

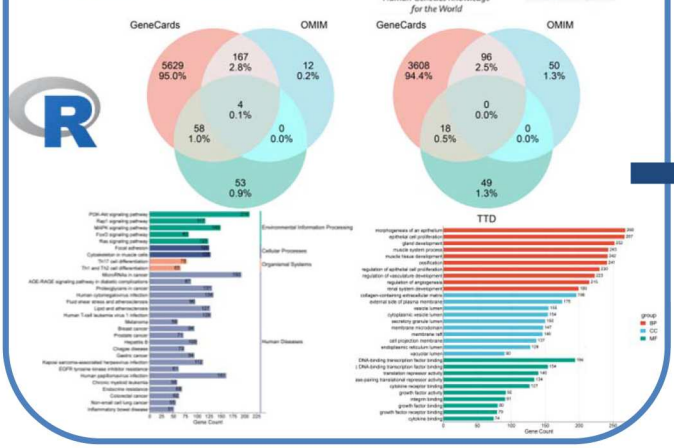
overlap of 7 hub genes derived from the Degree, EPC, MCC, and MNC algorithms in the CytoHubba plugin. PPI: Protein-protein interaction; MCODE: Molecular Complex Detection; EPC: Edge Percolated Component, MCC: Maximal Clique Centrality, and MNC: Maximum Neighborhood Component.

Fig. 5 The docking results between osimertinib and seven target proteins: (A) HDAC1, (B) CREBBP, (C) HDAC2, (D) EP300, (E) TP53, (F) SMARCA4, and (G) ESR1. Osimertinib was displayed in yellow, while the target proteins were shown in blue.

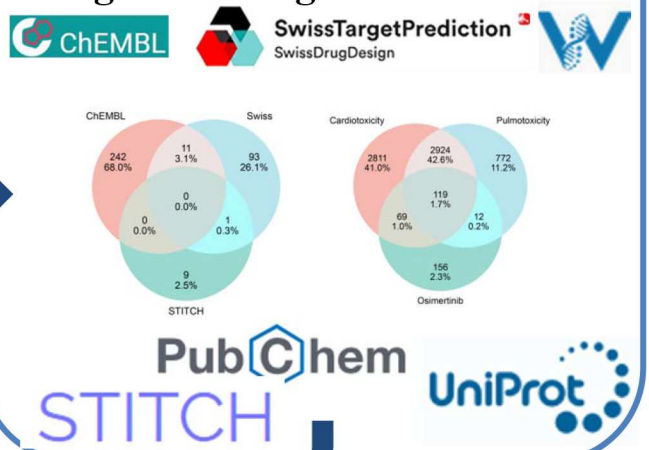
Fig. 6MDS of osimertinib with core target proteins. (A) RMSD analysis of 100 ns simulation of osimertinib with HDAC1 and CREBBP. (B) RMSF analysis of 100 ns simulation of osimertinib with HDAC1 and CREBBP. (C) Rg analysis of osimertinib with HDAC1 and CREBBP. (D) SASA analysis of osimertinib with HDAC1 and CREBBP. (E) HB analysis of osimertinib with HDAC1 and CREBBP. RMSD: root mean square deviation; RMSF: root mean square fluctuation; Rg: Radius of gyration; SASA: Solvent accessible surface area; HB: hydrogen bonding.

Fig. 7 MDS of osimertinib with core target proteins. (A) The 2D and 3D free energy landscapes of osimertinib with HDAC1. (B) The 2D and 3D free energy landscapes of osimertinib with CREBBP. (C) The MMPBSA binding free energies of osimertinib with HDAC1 and CREBBP. (D) Amino acid residue energy decomposition of osimertinib with HDAC1 and CREBBP. MMPBSA: Molecular Mechanics Poisson-Boltzmann Surface Area; $E_{VDWAALS}$: the energy of Van der Waals force; $E_{EL}$: Electrostatic Energy of interaction; $E_{PB}$: Electrostatic Polarization Born; $E_{NPOLAR}$: Nonpolar Solvation Free Energy; $G_{GAS}$: Gas Phase Molecular Mechanics Energy; $G_{SOLV}$: Solvation Free Energy; $d_G$: Total Binding Free Energy.

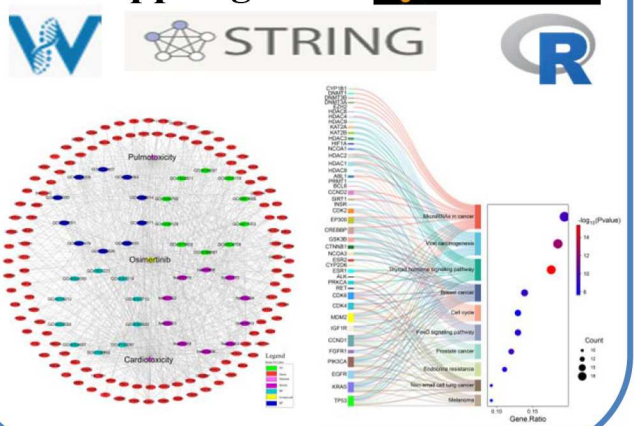
## Step1 Disease targets prediction



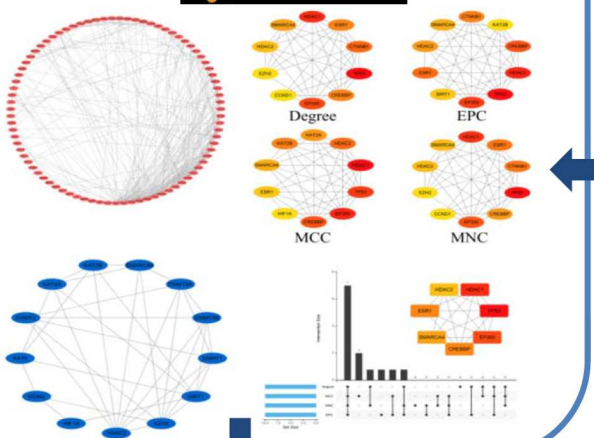

## Step2 Prediction of Common Targets of Drugs and Diseases



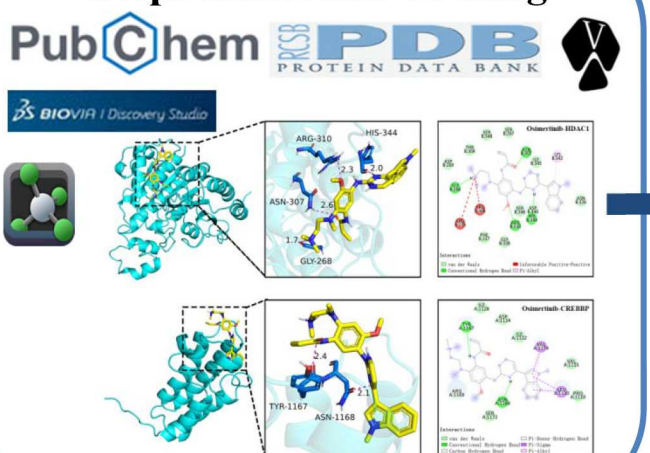

## Step3 Network construction of overlapped genes



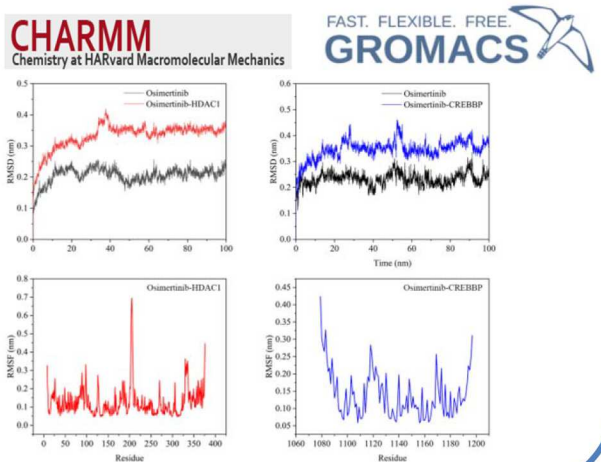

## Step4 Screening for hub genes

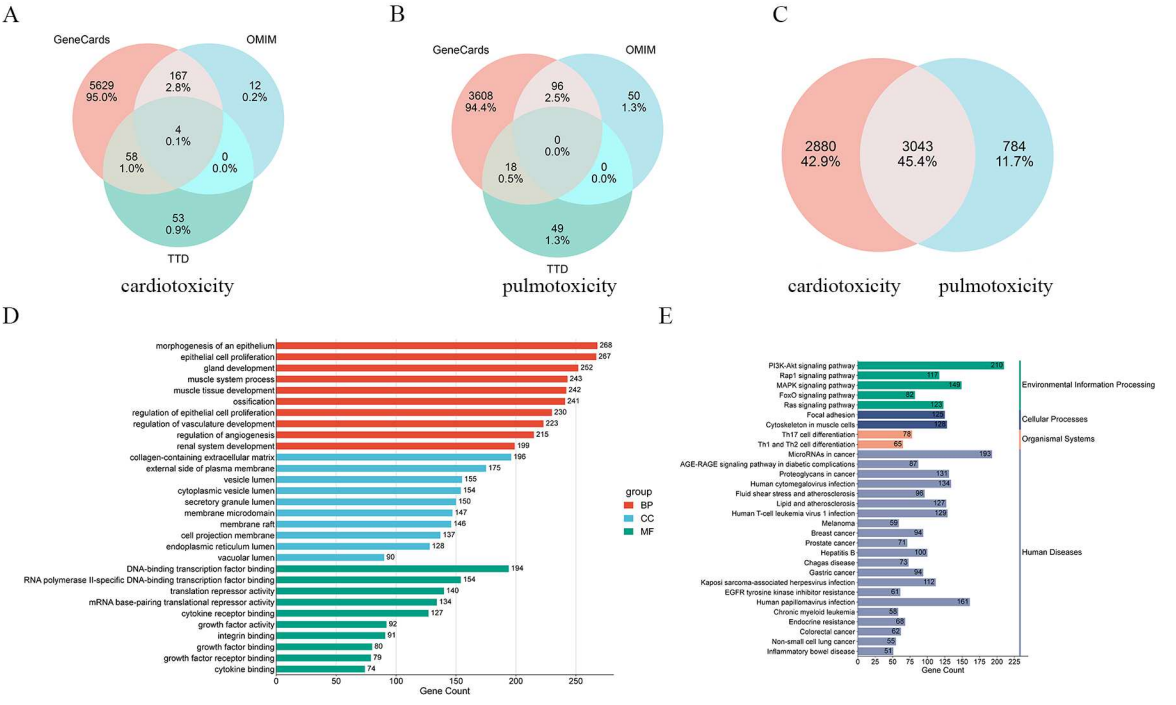


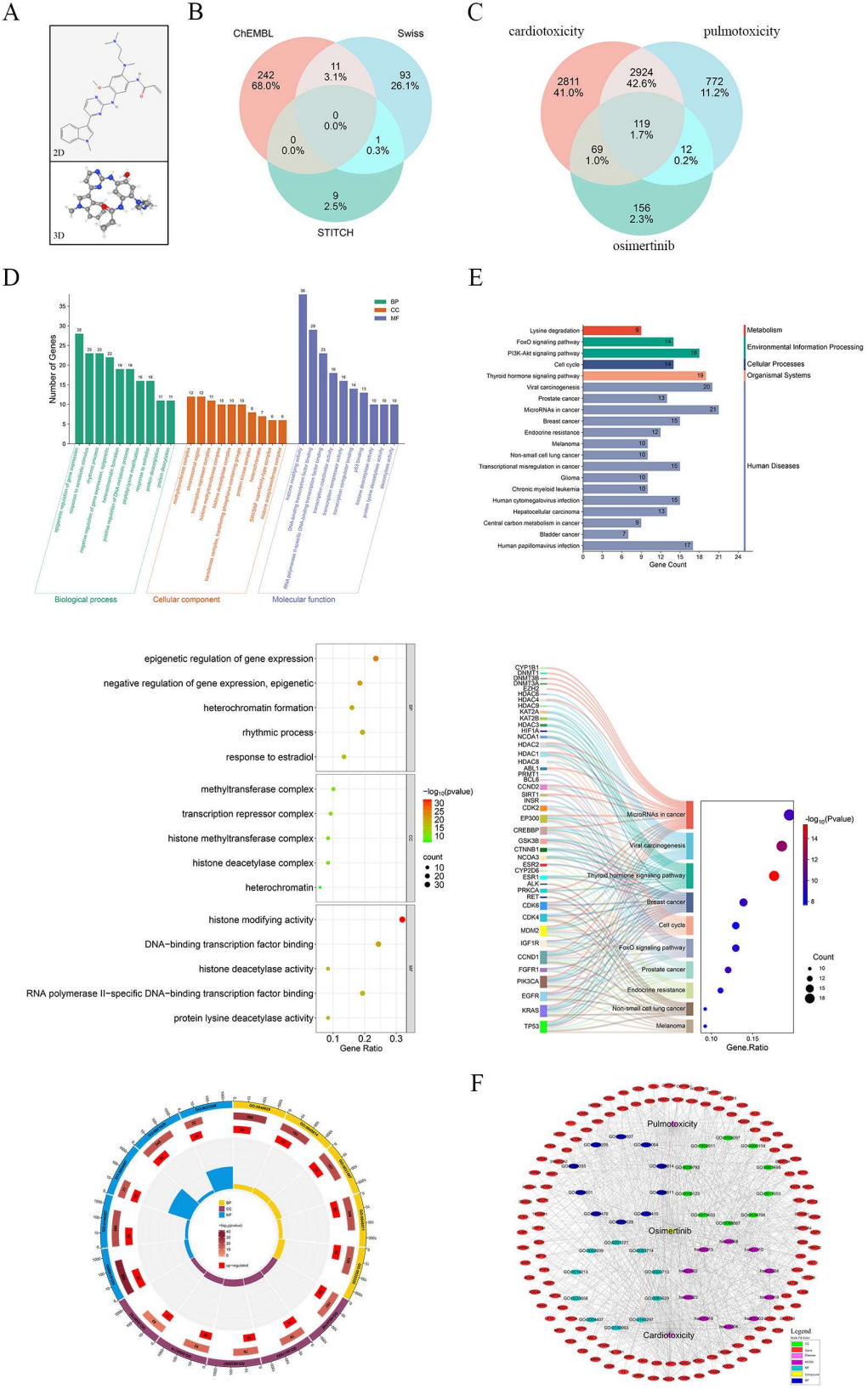

## Step5 Molecular docking

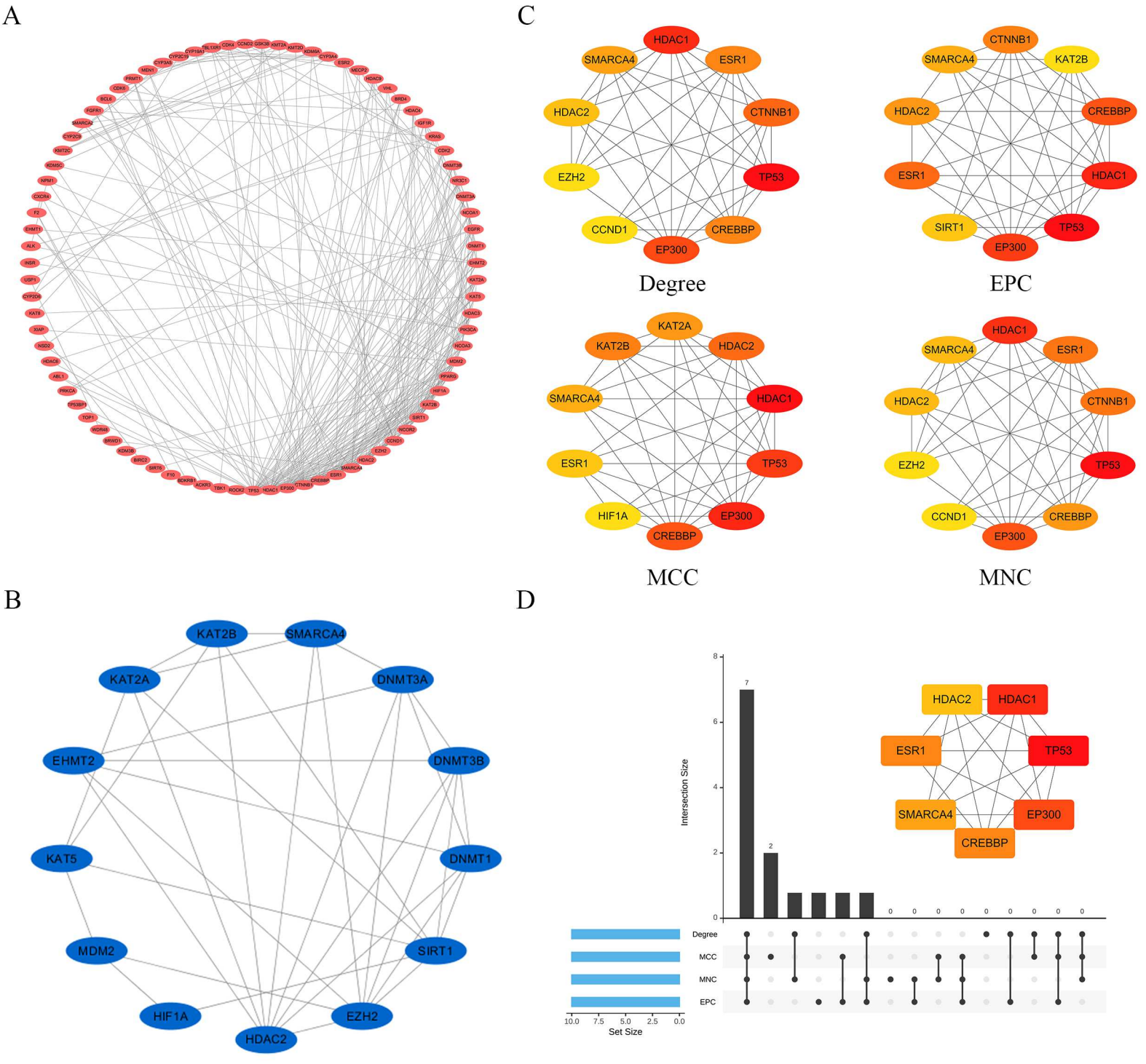


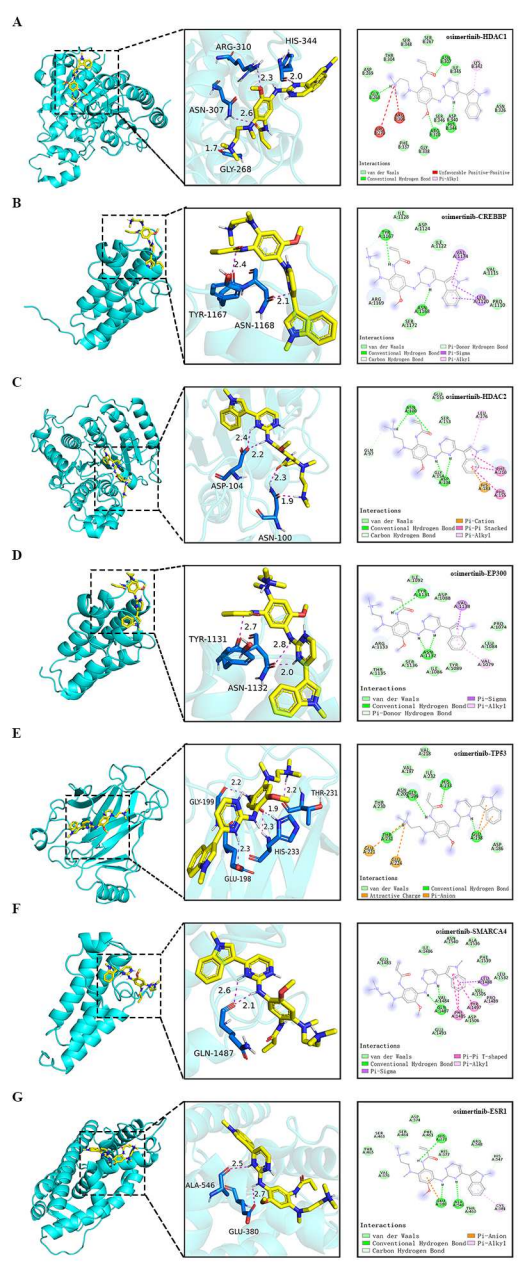

## Step6 Molecular dynamics

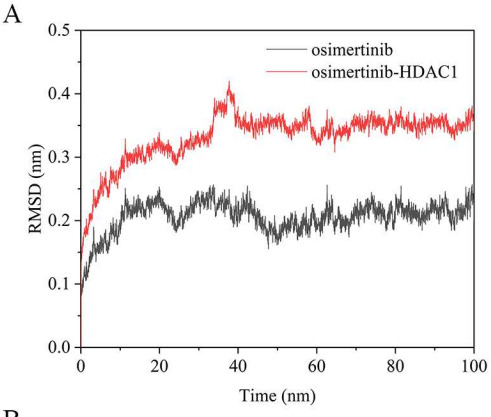


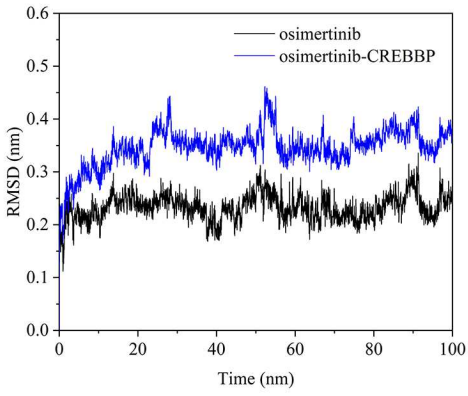

A
GeneCards
OMIM
TTD
5629
95.0%
167
2.8%
12
0.2%
4
0.1%
58
1.0%
0
0.0%
53
0.9%
cardiotoxicity
B
GeneCards
OMIM
TTD
3608
94.4%
96
2.5%
50
1.3%
0
0.0%
18
0.5%
0
0.0%
49
1.3%
pulmotoxicity
C
2880
42.9%
3043
45.4%
784
11.7%
cardiotoxicity
pulmotoxicity
D
morphogenesis of an epithelium 268
epithelial cell proliferation 267
gland development 252
muscle system process 243
muscle tissue development 242
ossification 241
regulation of epithelial cell proliferation 230
regulation of vasculature development 223
regulation of angiogenesis 215
renal system development 199
collagen-containing extracellular matrix 196
external side of plasma membrane 175
vesicle lumen 155
cytoplasmic vesicle lumen 154
secretory granule lumen 150
membrane microdomain 147
membrane raft 146
cell projection membrane 137
endoplasmic reticulum lumen 128
vacuolar lumen 90
DNA-binding transcription factor binding 194
RNA polymerase II-specific DNA-binding transcription factor binding 154
translation repressor activity 140
mRNA base-pairing translational repressor activity 134
cytokine receptor binding 127
growth factor activity 92
integrin binding 91
growth factor binding 80
growth factor receptor binding 79
cytokine binding 74
0 50 100 150 200 250
Gene Count
group
BP
CC
MF
E
PI3K-Akt signaling pathway 210
Rap1 signaling pathway 147
MAPK signaling pathway 146
FoxO signaling pathway 86
Ras signaling pathway 123
Focal adhesion 128
Cytoskeleton in muscle cells 110
Th17 cell differentiation 78
Th1 and Th2 cell differentiation 65
MicroRNAs in cancer 193
AGE-RAGE signaling pathway in diabetic complications 87
Proteoglycans in cancer 131
Human cytomegalovirus infection 134
Fluid shear stress and atherosclerosis 98
Lipid and atherosclerosis 127
Human T-cell leukemia virus 1 infection 129
Melanoma 59
Breast cancer 94
Prostate cancer 71
Hepatitis B 100
Chagas disease 73
Gastric cancer 94
Kaposi sarcoma-associated herpesvirus infection 112
EGFR tyrosine kinase inhibitor resistance 61
Human papillomavirus infection 161
Chronic myeloid leukemia 53
Endocrine resistance 68
Colorectal cancer 60
Non-small cell lung cancer 55
Inflammatory bowel disease 51
Environmental Information Processing
Cellular Processes
Organismal Systems
Human Diseases
0 25 50 75 100 125 150 175 200 225
Gene Count

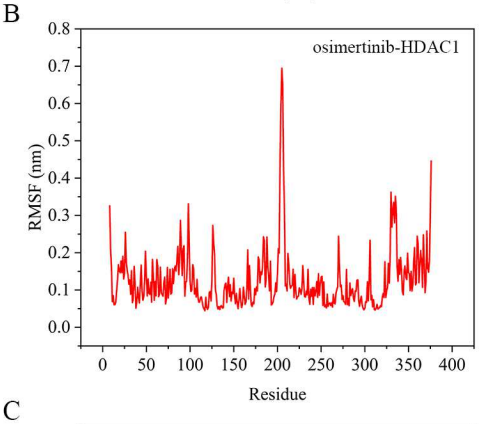

A
2D
3D
B
ChEMBL
Swiss
STITCH
242
68.0%
11
3.1%
93
26.1%
0
0.0%
0
0.0%
1
0.3%
9
2.5%
C
cardiotoxicity
pulmotoxicity
osimertinib
2811
41.0%
2924
42.6%
772
11.2%
119
1.7%
69
1.0%
12
0.2%
156
2.3%
D
Number of Genes
BP
CC
MF
Biological process
Cellular component
Molecular function
E
Lysine degradation
FoxO signaling pathway
PI3K-Akt signaling pathway
Cell cycle
Thyroid hormone signaling pathway
Viral carcinogenesis
Prostate cancer
MicroRNAs in cancer
Breast cancer
Endocrine resistance
Melanoma
Non-small cell lung cancer
Transcriptional misregulation in cancer
Glioma
Chronic myeloid leukemia
Human cytomegalovirus infection
Hepatocellular carcinoma
Central carbon metabolism in cancer
Bladder cancer
Human papillomavirus infection
Metabolism
Environmental Information Processing
Cellular Processes
Organismal Systems
Human Diseases
Gene Count
epigenetic regulation of gene expression
negative regulation of gene expression, epigenetic
heterochromatin formation
rhythmic process
response to estradiol
methyltransferase complex
transcription repressor complex
histone methyltransferase complex
histone deacetylase complex
heterochromatin
histone modifying activity
DNA−binding transcription factor binding
histone deacetylase activity
RNA polymerase II−specific DNA−binding transcription factor binding
protein lysine deacetylase activity
−log10(pvalue)
count
Gene Ratio
CYP1B1
DNMT1
DNMT3B
DNMT3A
EZH2
HDAC6
HDAC4
HDAC9
KAT2A
KAT2B
HDAC5
HIF1A
NCOA1
HDAC2
HDAC1
HDAC8
ABL1
PRKCI
BCL6
CCND2
SIRT1
INSR
CDK2
EP300
CREBBP
GSK3B
CTNNB1
NCOA3
ESR2
CYP2D6
ESR1
ALK
PRKCA
RET
CDK6
CDK4
MDM2
IGF1R
CCND1
FGFR1
PIK3CA
EGFR
KRAS
TP53
MicroRNAs in cancer
Viral carcinogenesis
Thyroid hormone signaling pathway
Breast cancer
Cell cycle
FoxO signaling pathway
Prostate cancer
Endocrine resistance
Non-small cell lung cancer
Melanoma
-log10(Pvalue)
Count
Gene.Ratio
F
Pulmotoxicity
Osimertinib
Cardiotoxicity
Legend

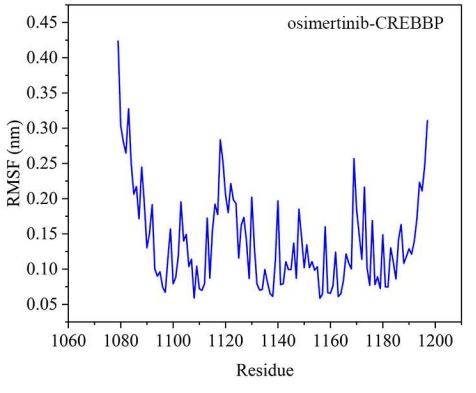

A
B
C
D
HDAC1
SMARCA4
ESR1
HDAC2
CTNNB1
EZH2
TP53
CCND1
CREBBP
EP300
Degree
CTNNB1
SMARCA4
KAT2B
HDAC2
CREBBP
ESR1
HDAC1
SIRT1
TP53
EP300
EPC
KAT2A
KAT2B
HDAC2
SMARCA4
HDAC1
ESR1
TP53
HIF1A
EP300
CREBBP
MCC
HDAC1
SMARCA4
ESR1
HDAC2
CTNNB1
EZH2
TP53
CCND1
CREBBP
EP300
MNC
KAT2B
SMARCA4
KAT2A
DNMT3A
EHMT2
DNMT3B
KAT5
DNMT1
MDM2
SIRT1
HIF1A
EZH2
HDAC2
Intersection Size
Set Size
Degree
MCC
MNC
EPC

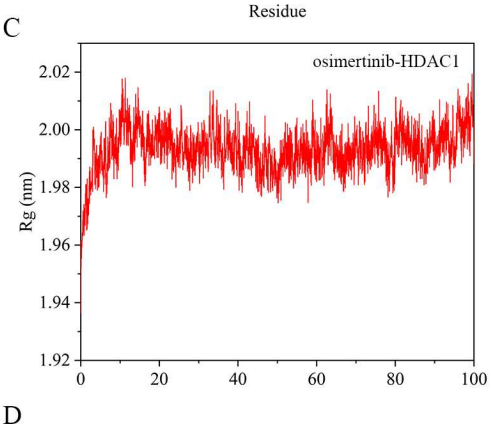

A
ARG-310
HIS-344
2.3
2.0
ASN-307
2.6
1.7
GLY-268
osimertinib-HDAC1
Interactions
van der Waals
Unfavorable Positive-Positive
Conventional Hydrogen Bond
Pi-Alkyl
B
2.4
2.1
TYR-1167
ASN-1168
osimertinib-CREBBP
Interactions
van der Waals
Pi-Donor Hydrogen Bond
Conventional Hydrogen Bond
Pi-Sigma
Carbon Hydrogen Bond
Pi-Alkyl
C
2.4
2.2
2.3
1.9
ASP-104
ASN-100
osimertinib-HDAC2
Interactions
van der Waals
Pi-Cation
Conventional Hydrogen Bond
Pi-Pi Stacked
Carbon Hydrogen Bond
Pi-Alkyl
D
2.7
2.8
2.0
TYR-1131
ASN-1132
osimertinib-EP300
Interactions
van der Waals
Pi-Sigma
Conventional Hydrogen Bond
Pi-Alkyl
Pi-Donor Hydrogen Bond
E
2.2
2.2
1.9
2.3
2.3
GLY-199
THR-231
HIS-233
GLU-198
osimertinib-TP53
Interactions
van der Waals
Conventional Hydrogen Bond
Attractive Charge
Pi-Anion
F
2.6
2.1
GLN-1487
osimertinib-SMARCA4
Interactions
van der Waals
Pi-Pi T-shaped
Conventional Hydrogen Bond
Pi-Alkyl
Pi-Sigma
G
2.5
2.7
ALA-546
GLU-380
osimertinib-ESR1
Interactions
van der Waals
Pi-Anion
Conventional Hydrogen Bond
Pi-Alkyl
Carbon Hydrogen Bond

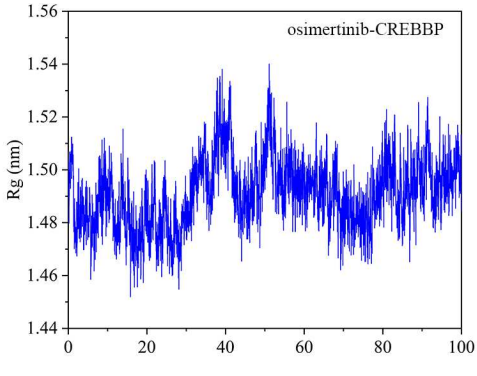

A
osimertinib
osimertinib-HDAC1
RMSD (nm)
Time (nm)

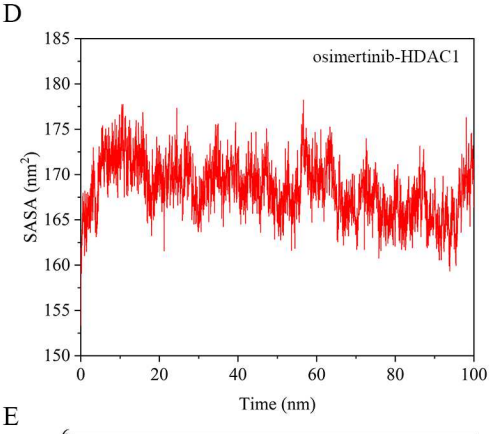

osimertinib
osimertinib-CREBBP
RMSD (nm)
Time (nm)

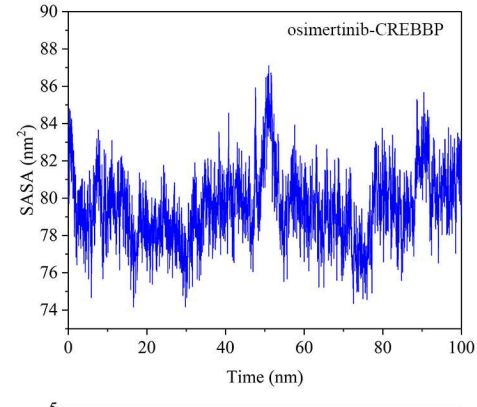

B
osimertinib-HDAC1
RMSF (nm)
Residue

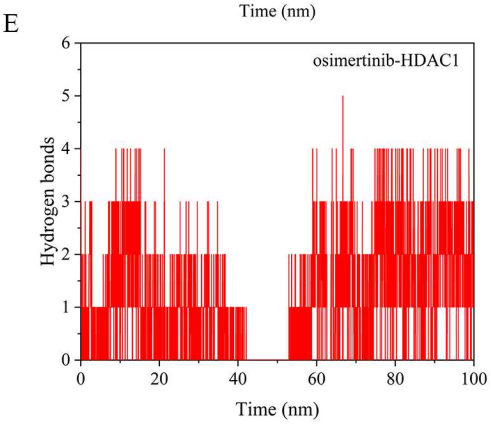

osimertinib-CREBBP
RMSF (nm)
Residue

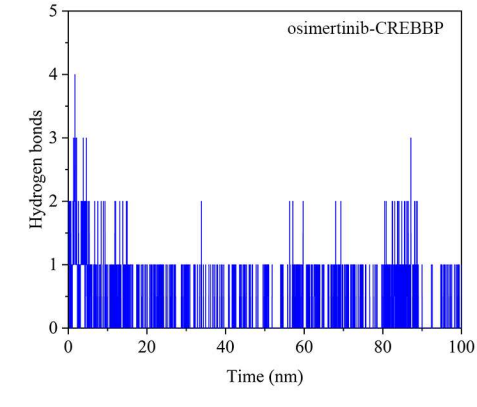

C
osimertinib-HDAC1
Rg (nm)


osimertinib-CREBBP
Rg (nm)

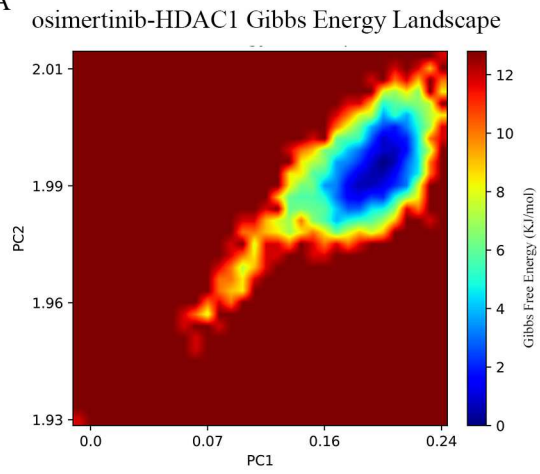

D
osimertinib-HDAC1
SASA (nm²)
Time (nm)

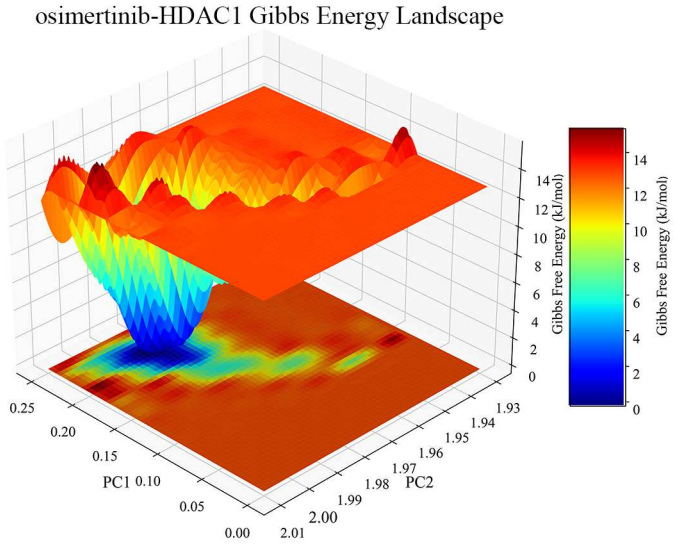

osimertinib-CREBBP
SASA (nm²)
Time (nm)


E
osimertinib-HDAC1
Hydrogen bonds
Time (nm)

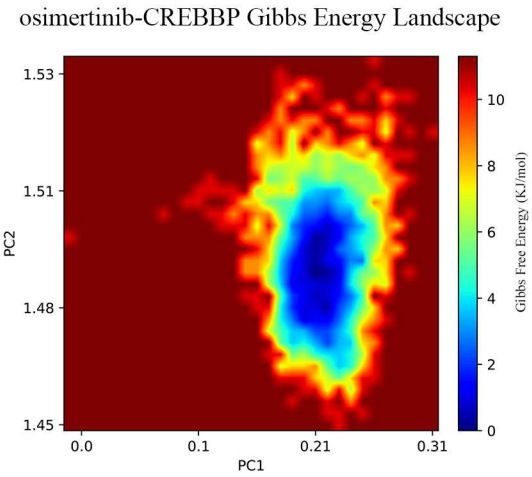

osimertinib-CREBBP
Hydrogen bonds
Time (nm)

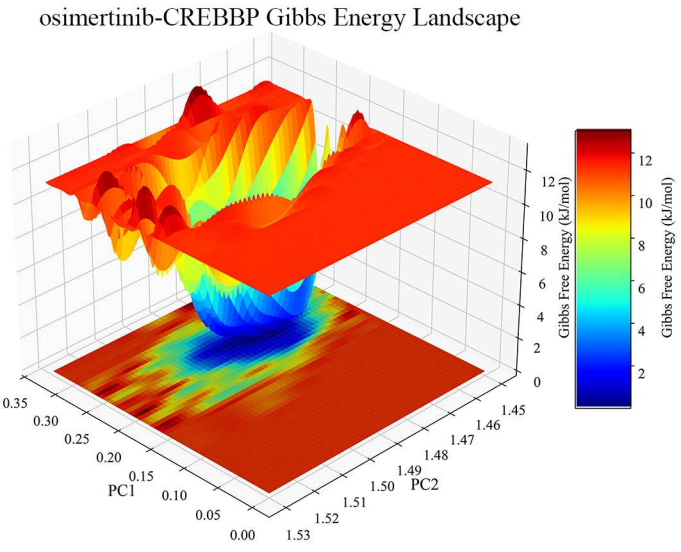
A


osimertinib-HDAC1 Gibbs Energy Landscape
PC2
PC1
Gibbs Free Energy (KJ/mol)

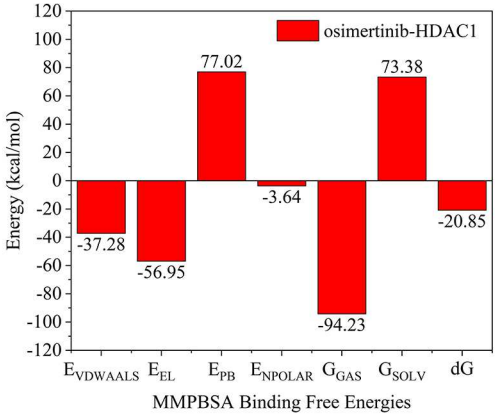

osimertinib-HDAC1 Gibbs Energy Landscape
PC1
PC2
Gibbs Free Energy (kJ/mol)

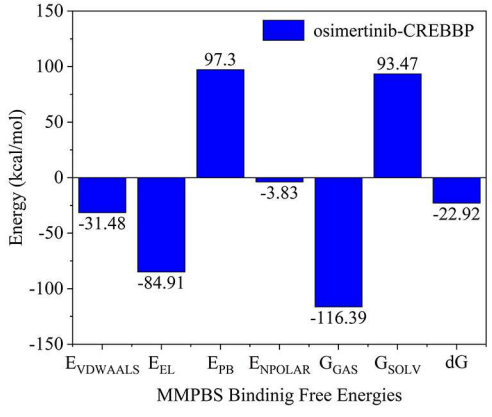
B


osimertinib-CREBBP Gibbs Energy Landscape
PC2
PC1
Gibbs Free Energy (KJ/mol)

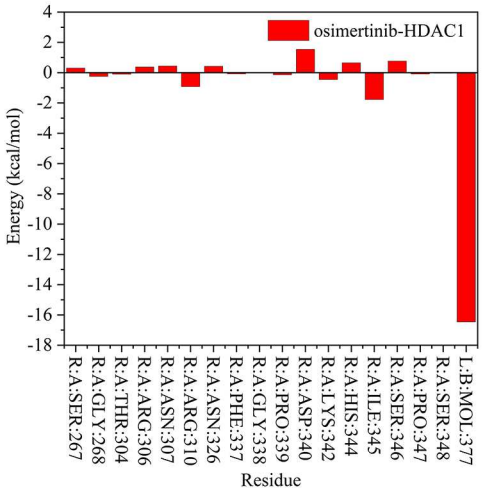

osimertinib-CREBBP Gibbs Energy Landscape
PC1
PC2
Gibbs Free Energy (kJ/mol)

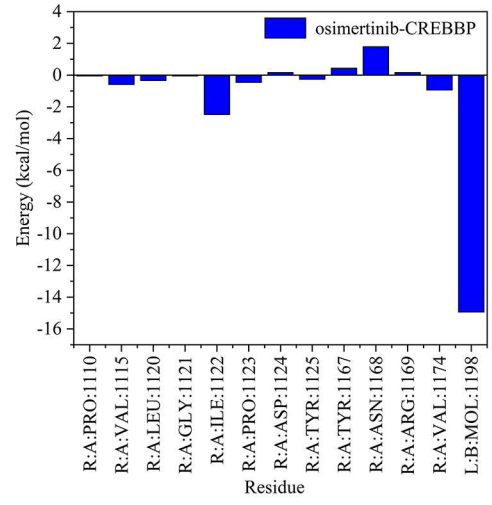
C


osimertinib-HDAC1
Energy (kcal/mol)
-37.28
-56.95
77.02
-3.64
-94.23
73.38
-20.85
E_VDWAALS E_EL E_PB E_NPOLAR G_GAS G_SOLV dG
MMPBSA Binding Free Energies


osimertinib-CREBBP
Energy (kcal/mol)
-31.48
-84.91
97.3
-3.83
-116.39
93.47
-22.92
E_VDWAALS E_EL E_PB E_NPOLAR G_GAS G_SOLV dG
MMPBS Bindinig Free Energies

D


osimertinib-HDAC1
Energy (kcal/mol)
R:A:SER:267
R:A:GLY:268
R:A:THR:304
R:A:ARG:306
R:A:ASN:307
R:A:ARG:310
R:A:ASN:326
R:A:PHE:337
R:A:GLY:338
R:A:PRO:339
R:A:ASP:340
R:A:LYS:342
R:A:HIS:344
R:A:ILE:345
R:A:SER:346
R:A:PRO:347
R:A:SER:348
L:B:MOL:377
Residue


osimertinib-CREBBP
Energy (kcal/mol)
R:A:PRO:1110
R:A:VAL:1115
R:A:LEU:1120
R:A:GLY:1121
R:A:ILE:1122
R:A:PRO:1123
R:A:ASP:1124
R:A:TYR:1125
R:A:TYR:1167
R:A:ASN:1168
R:A:ARG:1169
R:A:VAL:1174
L:B:MOL:1198
Residue

## Supplementary Files

This is a list of supplementary files associated with this preprint. Click to download.

- supplementaryMethods.docx
- SupplementaryTableS1.xlsx
- SupplementaryTableS2.xlsx
- SupplementaryTableS3.xlsx
- SupplementaryTableS4.xlsx
- SupplementaryTableS5.xlsx
- SupplementaryTableS5.xlsx
- SupplementaryTableS6.xlsx
- SupplementaryTableS7.xlsx
- SupplementaryTableS8.xlsx